

Original Research

# Mechanism of Gynecological Tiaoqi Jiedu Formula in Treatment of Endometritis with Dampness and Heat: A Prospective Laboratory-Based Mice Model Study

Jixiang Chen<sup>1,†</sup>, Chuanmei Zhong<sup>2</sup>, Wensi Yu<sup>2</sup>, Yan Lv<sup>3,†</sup>, Ning Li<sup>4,\*</sup><sup>1</sup>Department of Obstetrics and Gynecology, Nanning Second Maternal and Child Health Hospital, 530001 Nanning, Guangxi, China<sup>2</sup>Department of Gynecology, Guangxi University of Chinese Medicine, 530001 Nanning, Guangxi, China<sup>3</sup>Department of Obstetrics and Gynecology, Songzi Maternal and Child Health Hospital, 434200 Jinzhou, Hubei, China<sup>4</sup>Department of Gynecology, Guangxi International Zhuang Medical Hospital Affiliated to Guangxi University of Chinese Medicine, 530001 Nanning, Guangxi, China\*Correspondence: [Lining0771@outlook.com](mailto:Lining0771@outlook.com) (Ning Li)

†These authors contributed equally.

Academic Editor: Michael H. Dahan

Submitted: 5 July 2023 Revised: 17 August 2023 Accepted: 22 August 2023 Published: 29 December 2023

## Abstract

**Background:** Endometritis is a common gynecological disease characterized by inflammation of the endometrium. The gynecological Tiaoqi Jiedu formula has been widely used to treat endometritis with dampness and heat. However, the mechanism of action remains unclear. **Methods:** A mouse model of endometritis with dampness and heat was established. The pathological changes of the uterus and tongue were detected by hematoxylin and eosin (HE) staining. Gastric aquaporin 3 (AQP3) and uterine cluster of differentiation 14 (CD14) protein were detected by immunohistochemistry. Concentrations of serum inflammatory factors interleukin-6 (IL-6), IL-1 $\beta$ , tumor necrosis factor  $\alpha$  (TNF- $\alpha$ ), IL-10, and IL-8 were measured by enzyme-linked immunosorbent assay (ELISA). The mRNA levels and protein expressions of nucleotide binding oligomerization domain- (NOD-), leucine-rich repeat- (LRR-) and NOD-like receptor thermal protein domain associated protein 3 (NLRP3), gasdermin D (GSDMD), caspase-1, toll-like receptor 4 (TLR4), p65, and phosphorylation of p65 (p-p65) were determined by real-time polymerase chain reaction (PCR) and Western Blot, respectively. **Results:** In the mouse model of endometritis, the medium- and high-doses of Tiaoqi Jiedu formula, and western medicine significantly downregulated the inflammatory factors IL-6, IL-1 $\beta$ , TNF- $\alpha$ , and IL-8. It upregulated the anti-inflammatory factor IL-10, and inhibited pyroptosis and the expression of key proteins in the TLR4/nuclear factor- $\kappa$ B (NF- $\kappa$ B) signaling pathway. **Conclusions:** The Tiaoqi Jiedu formula demonstrated anti-inflammatory, anti-pyroptosis, and protective effects in endometritis. It has the potential to be a therapeutic option for the treatment of endometritis.

**Keywords:** endometritis; gynecology; Tiaoqi Jiedu formula; lipopolysaccharide; inflammatory factors; animal studies

## 1. Introduction

Chronic endometritis (CE) is a persistent inflammatory disease that is characterized by mucosal interstitial edema, focal or diffuse congestion, endometrial polyps, and interstitial plasma cell infiltration [1]. The prevalence of CE in infertile women varies between 2.8% to 56.8%, and it is associated with adverse pregnancy outcomes and endometriosis [2–5]. This disease has a significant impact on the health and quality of life of women and imposes a substantial economic burden on society. Currently, there are no universally accepted standardized diagnostic guidelines or treatment protocols for CE [6,7]. Therefore, there is a pressing need to investigate the pathogenesis of endometritis to develop effective treatment options that can improve pregnancy rates.

Endometritis is a persistent inflammatory disease with a prevalence of 2.8–56.8% in infertile women and is related to adverse pregnancy outcomes [3,8]. Traditional Chinese medicine (TCM) classifies CE as a dampness and heat syn-

drome and emphasizes the importance of tonifying Qi and nourishing blood, clearing away heat and detoxification, promoting water, and seeping dampness [9,10]. Gynecological Tiaoqi Jiedu formula has been used for many years in gynecological clinics to treat endometritis with certain effects in improving menstruation and pregnancy rate. However, there is a lack of in-depth research on its biological basis and molecular mechanism. This study established a mouse model of endometritis with dampness and heat by simulating the TCM pathogenesis, and observed the molecular mechanism of gynecological Tiaoqi Jiedu formula, providing a theoretical basis for clinical medication. The results showed that the Tiaoqi Jiedu formula demonstrated anti-inflammatory, anti-pyroptosis, and protective effects in endometritis, indicating its potential as a therapeutic option for the treatment of CE.



## 2. Material and Method

### 2.1 Experimental Materials

#### 2.1.1 Animals

Experimental animals were treated in accordance with the Animal Quality Management Measures, issued by the State Science and Technology Commission. Specific pathogen free (SPF) grade Kunming female mice of 8 weeks, with an average weight of 30–35 g, were purchased from Changsha Tianqin Biotechnology Co., Ltd., with animal certificate number 43072620100069835, and production license number SCXK (Xiang) 2019-0014.

#### 2.1.2 Animal Diets

The animal experimental center of Guangxi University of Traditional Chinese Medicine (Guangxi, China) processed a high-fat and high-sugar diet in accordance with standardized diagnostic guidelines or treatment protocols. The formula ratio consisted of 60% standard chow, 12% palm oil, 18% sucrose, 3% cholesterol, and 7% egg yolk powder. Additionally, the animal experiment center provided a common feed standard diet.

#### 2.1.3 Drugs

The formula for gynecological Tiaoqi Jiedu is composed of: 15 g Huanghua Ddaoshuilian, 15 g Wuzhi Maotao, 30 g Baizhu fried with bran, 30 g Shanyao, 15 g Jiubiyang, 15 g Tufuling, 15 g Buzhaye, 10 g Bijie, 15 g Cangzhu fried with bran, 6 g Baishao, 9 g Cheqianzi (bagged by cloth), 3 g Chaihu, 3 g Jingjiesui, 6 g Gancao, and 5 g Chenpi. The Chinese herbs should be decocted into three concentrations: 50 mL, 100 mL, and 200 mL, which are provided by the preparation department of the international Zhuang Medical Hospital, affiliated with Guangxi University of Traditional Chinese Medicine. Levofloxacin hydrochloride (HCl) tablets (100 mg) were supplied by Zhejiang Jingxin Pharmaceutical Co., Ltd. (Shaoxing, Zhejiang, China) (Approval number SFDAH1990060).

#### 2.1.4 Reagents

100 mg lipopolysaccharide (LPS, L2630, Bioswamp, Wuhan, Hubei, China), human myeloperoxidase (MPO) enzyme-linked immunosorbent assay (ELISA) Kit (batch No.: MU30238, Bioswamp, Wuhan, Hubei, China), interleukin 6 (IL-6) ELISA Kit (batch No.: MU30044, Bioswamp, Wuhan, Hubei, China), IL-1 $\beta$  ELISA Kit (batch No.: MU30369, Bioswamp, Wuhan, Hubei, China), protein quantification kit (batch No.: BL521A-1, Biosharp, Wuhan, Hubei, China), rabbit anti-toll-like receptor 4 (TLR4) antibody, rabbit anti-nuclear factor- $\kappa$ B (NF- $\kappa$ B) p65 polyclonal antibody, p-NF- $\kappa$ B p65 polyclonal antibody, anti-cysteine-aspartic acid protease (CASP1) polyclonal antibody, anti-gasdermin D (GSDMD) rabbit polyclonal antibody, anti-nucleotide binding oligomerization domain- (NOD-), leucine-rich repeat- (LRR-) and pyrin

domain-containing protein 3 (NLRP3) polyclonal antibody, rabbit anti-caspase-1p20 polyclonal antibody (batch No.: K003881P, K003407P, K006209P, K107599P, K006296P, K004108P, bs-10743R, Solarbio, Beijing, China), goat anti-rabbit immunoglobulin G (IgG) (batch No.: BL003a, Biosharp, Wuhan, Hubei, China), ECL chemiluminescent substrate kit (batch No.: BL523A, Biosharp, Wuhan, Hubei, China), 10% SDS-PAGE gel SuperQuick preparation kit (Sericebio batch No.: G2043-50T, Wuhan, Hebei, China), Quantitative Polymerase Chain Reaction (PCR) kit (Novabio, batch No.: Q204, Périgueux, France), reverse transcription kit (batch No.: R202, Novabio, Périgueux, France), and total RNA extraction kit (Tiangen, batch No.: DP424, Beijing, China) were used in this studies.

#### 2.1.5 Experimental Instruments

The instruments used in this study were a high-speed tissue grinder with low temperature (Wuhan Servicebio Biotechnology Co., Ltd., Wuhan, Hebei, China), a SIM-F140AY65-PC ice maker machine (Panasonic, Osaka, Japan), a PowerPac™ Basic Power Supply (Bio-Rad company, Hercules, CA, USA), a FluorChem E system (Protein Simple Co., Ltd., Tokyo, Japan), a 5430R high-speed freezing centrifuge (Eppendorf China Ltd., Beijing, China), a DW-86-L290-80oC pathological slicer (Shanghai Leica Instrument Co., Ltd., Shanghai, China), a film spreading machine (Zhejiang Kedi Instrument Equipment Co., Ltd., KDP, Jinhua, Zhejiang, China), a microscope (Nikon E100, Tokyo, Japan), an imaging system (Nikon DS-U3, Tokyo, Japan), a Light Cycler 96 automatic real-time fluorescent quantitative PCR instrument (Roche, Basel, Switzerland), and an Infinite m200 Pro multi-functional microplate detector and microplate reader (TECAN Trading Co., Ltd., Shanghai, China).

## 2.2 Methods

### 2.2.1 Animal Groups

After a week of adaptive feeding, ten mice were randomly selected for the control group, and the remaining fifty mice were used for the model of endometritis (with dampness and heat). The mice were evaluated according to references and were randomly divided into the model group, low-dose group, medium-dose group, high-dose group, and levofloxacin hydrochloride (HCl) group.

### 2.2.2 Model

2.2.2.1 Syndrome Model Establishment. In the control group, the animals were kept in a SPF grade laboratory room with standard diet and water at 20–25 °C and 50–60% humidity for 28 days. In the dampness and heat model group, the animals were kept in an artificial climate box at 30  $\pm$  0.15 °C and a humidity of 80–90% for 8 hours (10:00–18:00) every day [11]. The animals were fed with high-fat and high-sugar diet every day, and white liquor was poured every other day (56° white liquor: the dilution

ratio of drinking water is 120:100, 0.5 mL/100 g). Physical changes were measured every week, and the syndrome mode was evaluated after 28 days.

**2.2.2.2 Drug Intervention.** On day 28, the mice in the control and model groups were administered normal saline daily. The low-, medium-, and high high-dose groups of gynecological Tiaoqi Jiedu Formula formula were given 0.37 mL each time, according to body weight, twice a day. In the western medicine group, the levofloxacin hydrochloride HCl tablets were crushed and diluted to 18 mg/mL with normal saline. According to body weight, 3.6 mg (0.2 mL) was used each time, once a day. All drugs were administered intragastrically, continuously for 5 days.

**2.2.2.3 Endometritis Model Establishment.** One hour after the last gavage, sodium pentobarbital (40–70 mg/kg) was injected intraperitoneally. The skin was prepared and disinfected, and the uterus was located by entering the abdomen from the position slightly below the renal area. 25  $\mu$ L of LPS (2.5  $\mu$ g/ $\mu$ L) was injected using a microsyringe into the uterine cavity. The control group was not specially treated. After 24 hours, blood was collected from the eyeballs, and the mice were sacrificed by cervical dislocation. The relevant samples were collected, and the indexes were determined [12,13].

### 2.3 Index Detection

#### 2.3.1 Pathological Examination of Tongue Root and Uterus

The tissues of the tongue root, stomach, and uterus of the mice were fixed with 4% formaldehyde, followed by paraffin embedding, sectioning, and hematoxylin and eosin (HE) staining. The pathological changes of each group were observed under the microscope [14,15].

#### 2.3.2 Immunohistochemical Staining

The expression of gastric aquaporin 3 (AQP3) and uterine cluster of differentiation 14 (CD14) was detected using the Strept Avidin-Biotin Complex (SABC) method [16]. The sections were dewaxed with xylene, rinsed with a gradient of ethanol to water, and washed with distilled water for 5 minutes. Antigen retrieval was conducted for 8 minutes and washed three times (5 minutes each). The sections were then incubated with 3% hydrogen peroxide (version: 10011208, Sinopharm Group Chemical Reagent Co., Ltd., Shanghai, China) for 25 minutes, washed three times, and incubated with 3% bovine serum albumin (BSA) (version: GC305010, Sinopharm Group Chemical Reagent Co., Ltd., Shanghai, China) for 30 minutes. The primary antibody was incubated at 4 °C overnight, followed by three washes. The sections were then incubated with the secondary antibody for 50 minutes, followed by color development with diaminobenzidine (DAB) and stopped with distilled water. After counterstaining with hematoxylin (version: 1212,

Sinopharm Group Chemical Reagent Co., Ltd., Shanghai, China), the sections were dehydrated, made transparent, and neutral balsam was used to seal them. All tissues were observed under a microscope, and images were collected and analyzed.

#### 2.3.3 The Histological Analysis and Quantification

Digital pathological image analysis software based on artificial intelligence learning. Artificial intelligence (AI) deep learning principle is used to train algorithms based on massive data and integrate them into automated image analysis software. The specific process is as follows:

(1) Tracking: automatically locate and delineate the area to be measured along the tissue to be measured, and manually locate according to specific requirements;

(2) Color selection: according to Hue Saturation Intensity (HSI) automatic positive judgment, can be manually corrected according to the specific situation;

(3) Calculation: According to the requirement, the nucleus was located automatically by the software and cytoplasm range was expanded. Different parameters of the positive cells such as the quantity which range from weak to strong, cell rate, tissue area and integrated optical density (IOD) were calculated.

(4) Analysis: Gradually calculate the area to be tested at high power. After completion, each project is calculated automatically according to the original basic data and the algorithm formula to obtain the analysis results, and generate a report.

#### 2.3.4 ELISA

Blood from the eyeballs was collected and stored at –80 °C after centrifugation. The content of the serum inflammatory factors IL-6, IL-1 $\beta$ , TNF- $\alpha$ , IL-10, and IL-8 were detected and analyzed according to the ELISA kit protocol [17].

#### 2.3.5 Real-Time PCR

The total RNA from the mice uterine tissue was extracted using Trizol reagent (version: #DP424, Tiangen Biochemical Technology Co., Ltd., Beijing, China) and reversed into cDNA. The primer sequence was designed by Beijing Qingke Biotechnology Co., Ltd. (Beijing, China). The primers used are shown in Table 1. The primers for NLRP3, GSDMD, Caspase-1, TLR4, p65, phosphorylation of p65 (p-p65), and other reaction reagents were added to the reaction system according to the requirements of the fluorescent quantitative amplification kit. The reaction procedure consisted of pre-denaturation at 95 °C for 30 seconds, denaturation at 95 °C for 3–10 seconds, annealing extension at 60 °C for 10–30 seconds, and 40 cycles. Each sample was run in three wells. The data were statistically analyzed by the maximum second derivative method ( $2^{-\Delta\Delta C_t}$ ). The relative expression of mRNA was calculated with *glyceraldehyde-3-phosphate dehydrogenase (GAPDH)* as an internal parameter.

**Table 1. Primer sequence of *NLRP3*, *GSDMD*, *Caspase-1*, *TLR4*, *p65*, and *p-p65*.**

Gene	Sequences	Length (5'→3')
<i>NLRP3</i>	Forward primer	ATTACCCGCCCGAGAAAGG
	Reverse primer	TCGCAGCAAAGATCCACACAG
<i>GSDMD</i>	Forward primer	CCATCGGCCTTTGAGAAAGTG
	Reverse primer	ACACATGAATAACGGGGTTTCC
<i>Caspase-1</i>	Forward primer	ACAAGGCACGGGACCTATG
	Reverse primer	TCCCAGTCAGTCCTGGAAATG
<i>TLR4</i>	Forward primer	ATGGCATGGCTTACACCACC
	Reverse primer	GAGGCCAATTTGTCTCCACA
<i>p65</i>	Forward primer	GGAGGCATGTTCCGGTAGTGG
	Reverse primer	CCCTGCGTTGGATTTCGTG
<i>p-p65</i>	Forward primer	AGGCTTCTGGGCCTTATGTG
	Reverse primer	TGCTTCTCTCGCCAGGAATAC
<i>GAPDH</i>	Forward primer	CTGGGCTACACTGAGCACC
	Reverse primer	AAGTGGTCGTTGAGGGCAATG

*NLRP3*, NOD-, LRR- and pyrin domain-containing protein 3; *GSDMD*, gasdermin D; *TLR4*, toll-like receptor 4; *p-p65*, phosphorylation of *p65*; *GAPDH*, glyceraldehyde-3-phosphate dehydrogenase; *NOD*, anti-nucleotide binding oligomerization domain; *LRR*, leucine-rich repeat.

### 2.3.6 Western Blot

The fresh uterine tissue was ground with steel beads using radio immuno precipitation (RIPA) buffer (version: #R0010, Beijing Solaibao Technology Co., Ltd., Beijing, China) and phenylmethyl sulfonyl fluoride (PMDF) (Version: B0009, Suzhou Yake Technology Co., Ltd., Suzhou, Jiangsu, China), followed by centrifugation. After extracting the total proteins, the sodium dodecyl sulfate polyacrylamide gel electrophoresis (SDS-PAGE) (version: G2043-50T, Wuhan Cel Technology Co., Ltd., Beijing, China) was boiled for 5 minutes. The bicinchoninic acid (BCA) method was used to detect the protein concentration. The proteins were loaded into the electrophoresis system, with the upper gel electrophoresed at 80 volts and the lower gel at 120 volts. After electrophoresis, the proteins were transferred to the polyvinylidene fluoride (PVDF) membrane and washed with tris buffered saline-tween (TBST) (version: T1082, Beijing Solaibao Technology Co., Ltd., Beijing, China) for 10 minutes (3 times). The membranes were incubated in primary antibodies (*NLRP3*, *GSDMD*, *Caspase-1*, *p20*, *TLR4*, *p65*, *p-p65* ratio of 1:1000; ratio 1:2000 for *Caspase-1*,  $\beta$ -actin ratio 1:2000) with 5% skimmed milk powder in a shaker at 4 °C overnight, and washed with TBST for 10 minutes (3 times). In the next step, the membranes were incubated in the secondary antibodies (sheep anti-rabbit, dilution ratio 1:5000) for 1 hour at room temperature, and washed with TBST for 10 minutes (3 times).  $\beta$ -Actin was used as an internal control. In the final step, the membranes were treated with electrochemiluminescence (ECL) (version: BL523A-1 and BL523A-2, Lanjiek Science and technology biological Co., Ltd., Beijing, China) lumines-

cent solution for 1 minute to develop color. The photos were captured to calculate the relative gray value with Image J software (8.0.2 version, National Institute of Health, Bethesda, MD, USA) (<https://imagej.en.softonic.com/>).

### 2.4 Statistical Analysis

Three biological replicates were conducted for all experiments. The figures and the data analysis were performed with the software GraphPad Prism 8.0 (GraphPad Software, Inc., San Diego, CA, USA) and SPSS 17.0 statistical analysis software (IBM Corp., Armonk, NY, USA). One-way analysis of variance (ANOVA) and Tukey's post hoc test was performed after confirmation of normality test. Independent paired *t*-test was used for the comparison between the groups. The results were expressed as mean  $\pm$  standard error.  $p < 0.05$  was regarded as statistical significance.

## 3. Results

### 3.1 General Conditions of Model Mice

The mice in the control group showed good mental state, sensitive reactions, normal diet and drinking water, good hair luster, normal urination, and normal vaginal secretions (Fig. 1). Conversely, the mice in the induced model group (dampness heat syndrome model) displayed less activity, were listless with slow reactions, had dull hair, low dietary and drinking water intake, slow weight gain, dark purple lips, yellow and foul-smelling urine, loose stool, dirty around the anus, and increased vaginal secretions. After drug intervention in the mice with low- and medium-doses of gynecological Tiaoqi Jiedu formula, the body weight and appearance did not show significant changes ( $p > 0.05$ ) compared to induced model without treatment (model group) (Table 2). However, the group treated with high doses of gynecological Tiaoqi Jiedu formula and western medicine showed significant ( $p < 0.01$ ) improvement in body weight, and a decrease in vaginal secretions compared to the induced model without treatment (model group).

### 3.2 Pathological Changes in HE Staining of Tongue

The histopathology of the tongue mucosal tissues is shown in Fig. 2. The tongue mucosa of the control group was clear and distinct, with even and moderately arranged papillae density, and clear and orderly arranged muscle bundles of lamina propria (Fig. 2A). In comparison with the control group (Table 3), the model group showed increased thickness of the lingual papillae ( $p < 0.01$ ). Additionally, lingual papillae density was significantly increased ( $p < 0.01$ ) (Table 3), arrangement was uneven (Fig. 2B), and the connective tissue of the lamina propria was significantly damaged, with hyperemia and inflammatory cell infiltration characterized by deep color (Fig. 2B). The mucosal tissue of the tongue in the low-dose group showed no significant changes ( $p > 0.01$ ) compared to the model group (Table 3; Fig. 2). However, the mice treated with medium-

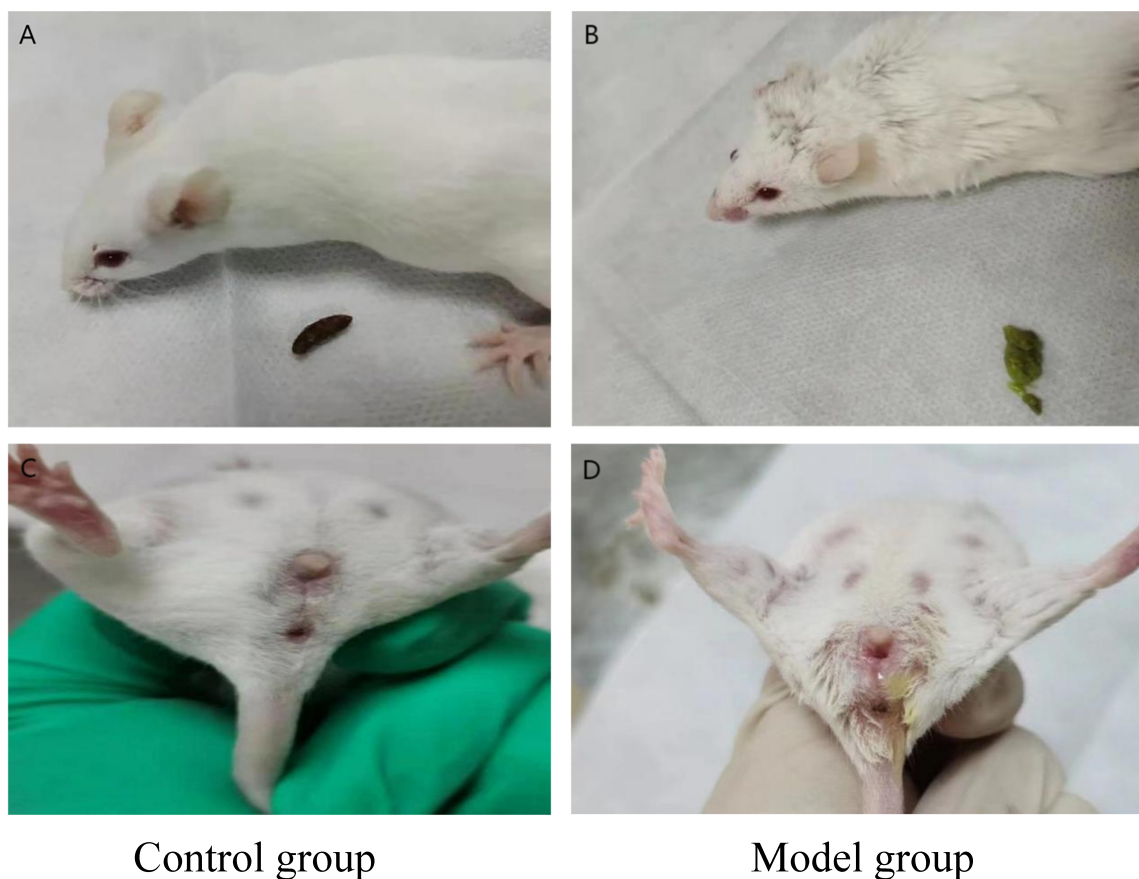


**Fig. 1.** Appearance of dampness heat syndrome in model group mice (B,D) compared to control group mice (A,C).

**Table 2.** Change in weight (physical parameter) of mice at different time intervals (n = 10, mean ± standard deviation).

Group	0 day (g)	7 days (g)	14 days (g)	21 days (g)	28 days (g)	33 days (g)
Control	32.6 ± 0.9	34.1 ± 0.9	35.6 ± 1.0	37.2 ± 0.9	38.5 ± 0.9	39.5 ± 0.8
Model	32.5 ± 0.9	33.9 ± 1.1	35.2 ± 0.9	36.0 ± 0.9 <sup>#</sup>	36.8 ± 1.1 <sup>#</sup>	37.4 ± 0.9 <sup>##</sup>
Low-dose	32.6 ± 0.7	34.1 ± 0.9	35.2 ± 0.9	36.9 ± 1.2	36.9 ± 1.2	37.4 ± 0.9
Medium-dose	32.7 ± 1.1	33.8 ± 1.1	35.1 ± 1.0	35.9 ± 0.9	36.8 ± 1.1	37.8 ± 1.1
High-dose	32.5 ± 1.1	33.8 ± 1.2	35.1 ± 1.1	36.1 ± 0.9	36.8 ± 1.2	38.6 ± 0.9 <sup>**</sup>
Western medicine	32.7 ± 1.1	33.9 ± 1.1	35.2 ± 1.1	36.1 ± 0.9	36.8 ± 1.1	38.6 ± 0.7 <sup>**</sup>

n, number. Compared with control group (<sup>#</sup> $p < 0.05$ , <sup>##</sup> $p < 0.01$ ). Compared with model group (<sup>\*\*</sup> $p < 0.01$ ).

, high-dose, and western medicine showed significant improvement ( $p < 0.01$ ) in the thickness of lingual papillae and the number of lingual papillae in the lamina propria (Table 3; Fig. 2). The high-dose and western medicine treated mice also showed improvement in the lamina propria, with low inflammatory cells, as expected (Table 3; Fig. 2).

### 3.3 Appearance of the Mice Uterus

In comparison to the control group (Fig. 3A), the uterine serous surface of the mice in the model group was congested and edematous (Fig. 3B). The color was dark red, the uterine diameter was about twice that of the control group, and the lumen was filled with pus (Fig. 3B). However, the swelling, congestion, and size of the uterus were

altered to different levels after treatment with gynecological Tiaoqi Jiedu formula (Fig. 3C–E), and western medicine group (Fig. 3F).

### 3.4 Histopathological Changes in the Mice Uterus

The mice uterus of the control group showed clear and complete layers of uterine endometrial epithelium and normal cell morphology. The number of uterine glands in the lamina propria was abundant and evenly distributed, and the myocytes in the myometrium were arranged regularly without obvious abnormalities (Fig. 4A). The mice uterus in the model group showed an uneven, thick endometrium, with a large number of epithelial cells, as a sign of necrosis. The nuclei were pyknosis, characterized by deep stain-

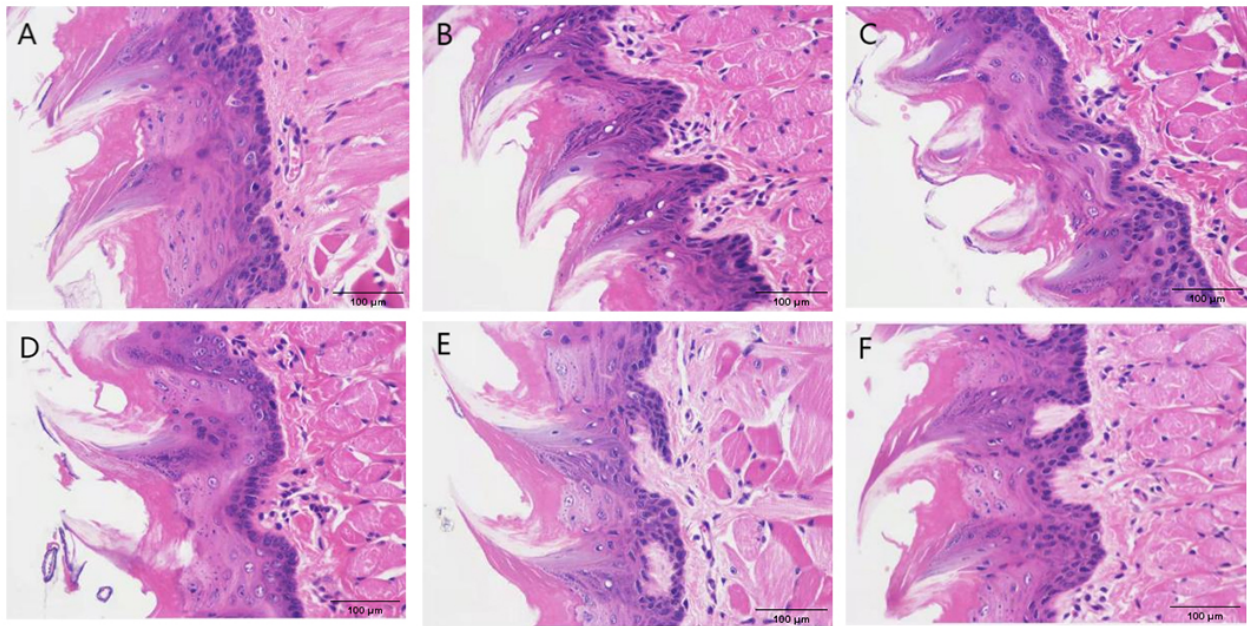


**Fig. 2. Histopathological images of tongue mucosal tissues.** (A) Control group. (B) Model group. (C) Low-dose group. (D) Medium-dose group. (E) High-dose group. (F) Levofloxacin hydrochloride (HCl) group.

**Table 3. Comparison of papillae density, mucosal epithelial thickness, and papillae number per unit length of lingual lamina propria (n = 6, mean ± standard deviation).**

Group	Number of lingual papillae of lamina propria	Thickness of lingual papillae (mm)	Number of lingual papillae per unit length (/mm)
Control	2.50 ± 0.55	0.44 ± 0.01	4.37 ± 0.09
Model	7.67 ± 0.82 <sup>##</sup>	0.51 ± 0.01 <sup>##</sup>	13.84 ± 0.97 <sup>##</sup>
Low-dose	7.63 ± 0.82	0.50 ± 0.02	13.49 ± 0.60
Medium-dose	5.00 ± 0.638 <sup>**</sup>	0.47 ± 0.01 <sup>**</sup>	10.76 ± 0.19 <sup>**</sup>
High-dose	3.83 ± 0.75 <sup>**</sup>	0.46 ± 0.01 <sup>**</sup>	6.48 ± 0.13 <sup>**</sup>
Western medicine	3.50 ± 0.84 <sup>**</sup>	0.47 ± 0.02 <sup>**</sup>	6.55 ± 0.12 <sup>**</sup>

Compared with control group (<sup>##</sup> $p < 0.01$ ). Compared with model group (<sup>\*\*</sup> $p < 0.01$ ).

ing, fragmentation, or dissolution (black arrow). A small number of epithelial cells of uterine glands in the lamina propria were necrotic, and the nuclei were pyknotic, hyperchromatic, fragmented, or dissolved (red arrows). A large amount of granulocyte infiltration could be seen in the lamina propria and muscularis of the intima (blue arrow) (Fig. 4B). The mice treated with a low- to high-doses of gynecological Tiaoqi Jiedu formula and levofloxacin HCl showed neutrophil infiltration, cytolysis, and fragmentation, which varied in different degrees in the lamina propria and muscularis of the inner membrane (Fig. 4C–F).

### 3.5 CD14 Expression in Mice Uterus

In regards to the immunohistochemical results, the brown staining of CD14 in the model group was deeper compared to the control group, indicating higher expression of CD14 (Fig. 5A,B). Next, in comparison to the model group (except for the low-dose group), the positive staining of CD14 in the treatment groups was reduced to varying de-

grees, as shown in Fig. 5C–F. The gray value of CD14 in the model group was significantly higher ( $p < 0.01$ ) compared to the control group. The gray value in the low-dose group did not change significantly when compared with the model mice. The gray value of CD14 in other treatment groups significantly decreased ( $p < 0.01$ ), as shown in Fig. 6.

### 3.6 AQP3 Expression in Mice Stomach

Regarding immunohistochemical results, a brownish yellow dot (positive) and sepia (strongly positive) represents AQP3 expression. Compared to the control group (Fig. 7A), the brown staining in the model group was deeper, which suggests higher expression of AQP3 (Fig. 7B). AQP3 expression in the low-dose treatment group (Fig. 7C) showed no change compared to the model group (Fig. 7B). The positive staining of AQP3 in other treatment groups was reduced to varying degrees, as shown in Fig. 7D–F.

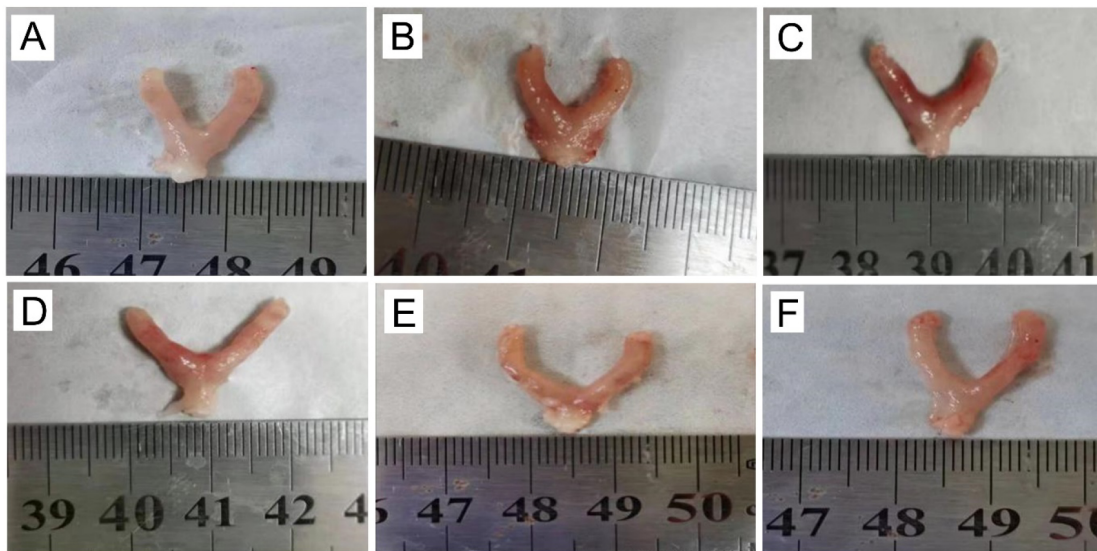


**Fig. 3. Appearance of uterus in mice.** (A) Control group. (B) Model group. (C) Low dose group. (D) Medium group. (E) High dose group. (F) Levofloxacin HCl group.

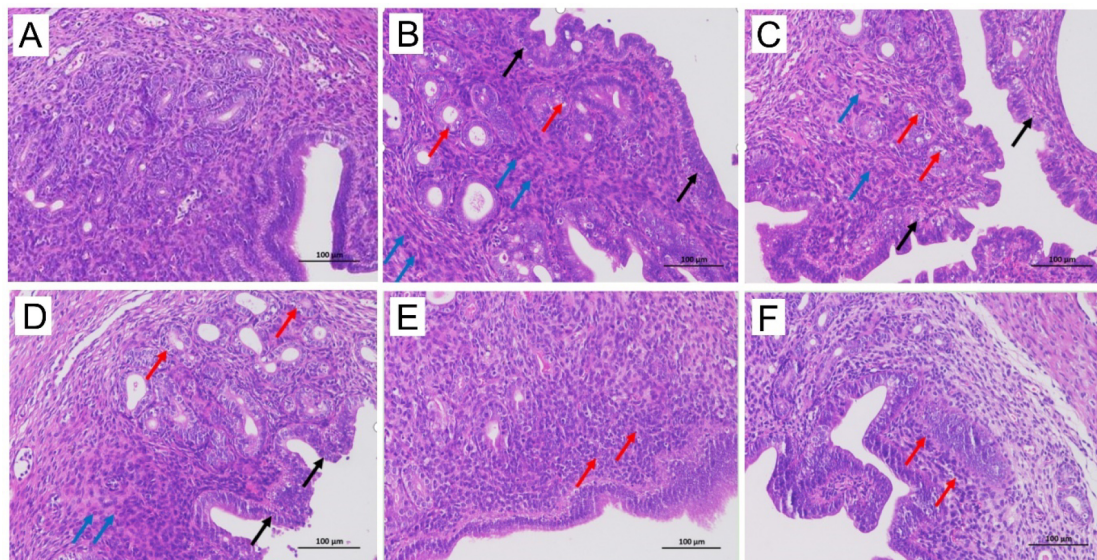


**Fig. 4. Histopathological images (200 $\times$ , scale bar is 100  $\mu$ m) of mice uterus.** (A) Control group. (B) Model group. (C) Low-dose group. (D) Medium-dose group. (E) High-dose group. (F) Levofloxacin HCl group. The black arrows represent a large number of epithelial cell necrosis, nuclear shrinkage, deep staining, fragmentation or dissolution; the red arrows represent a small number of necrotic uterine epithelial cells, nuclear shrinkage, deep staining, fragmentation or dissolution; the blue arrows represent neutrophils.

**Table 4. Level of serum inflammatory factors in mice (n = 6, mean  $\pm$  standard deviation).**

Group	IL-10	TNF- $\alpha$	IL-8	IL-6	IL-1 $\beta$
Control group	187.2 $\pm$ 11.5	105.5 $\pm$ 5.4	129.7 $\pm$ 5.3	23.5 $\pm$ 2.8	58.3 $\pm$ 3.7
Model group	132.8 $\pm$ 10.2 <sup>###</sup>	199.3 $\pm$ 7.0 <sup>###</sup>	208.9 $\pm$ 30.9 <sup>###</sup>	66.1 $\pm$ 4.4 <sup>##</sup>	152.0 $\pm$ 5.6 <sup>##</sup>
Low-dose group	134.6 $\pm$ 6.6	197.7 $\pm$ 6.2	204.0 $\pm$ 12.9	63.3 $\pm$ 2.3*	146.0 $\pm$ 3.7
Medium-dose group	141.9 $\pm$ 10.3	164.3 $\pm$ 9.2 <sup>***</sup>	184.2 $\pm$ 5.8 <sup>***</sup>	48.4 $\pm$ 1.2 <sup>**</sup>	129.5 $\pm$ 6.1 <sup>**</sup>
High-dose group	167.9 $\pm$ 12.2 <sup>***</sup>	122.4 $\pm$ 4.9 <sup>***</sup>	158.8 $\pm$ 5.7 <sup>***</sup>	32.3 $\pm$ 1.4 <sup>**</sup>	63.2 $\pm$ 5.3 <sup>**</sup>
Western medicine	169.7 $\pm$ 9.7 <sup>***</sup>	126.3 $\pm$ 6.3 <sup>***</sup>	155.6 $\pm$ 9.3 <sup>***</sup>	32.5 $\pm$ 0.7 <sup>**</sup>	64.4 $\pm$ 3.9 <sup>**</sup>

Compared with control group (<sup>##</sup> $p < 0.01$ , <sup>###</sup> $p < 0.001$ ). Compared with model group (<sup>\*</sup> $p < 0.05$ , <sup>\*\*</sup> $p < 0.01$  and <sup>\*\*\*</sup> $p < 0.001$ ). IL, interleukin; TNF, tumor necrosis factor.

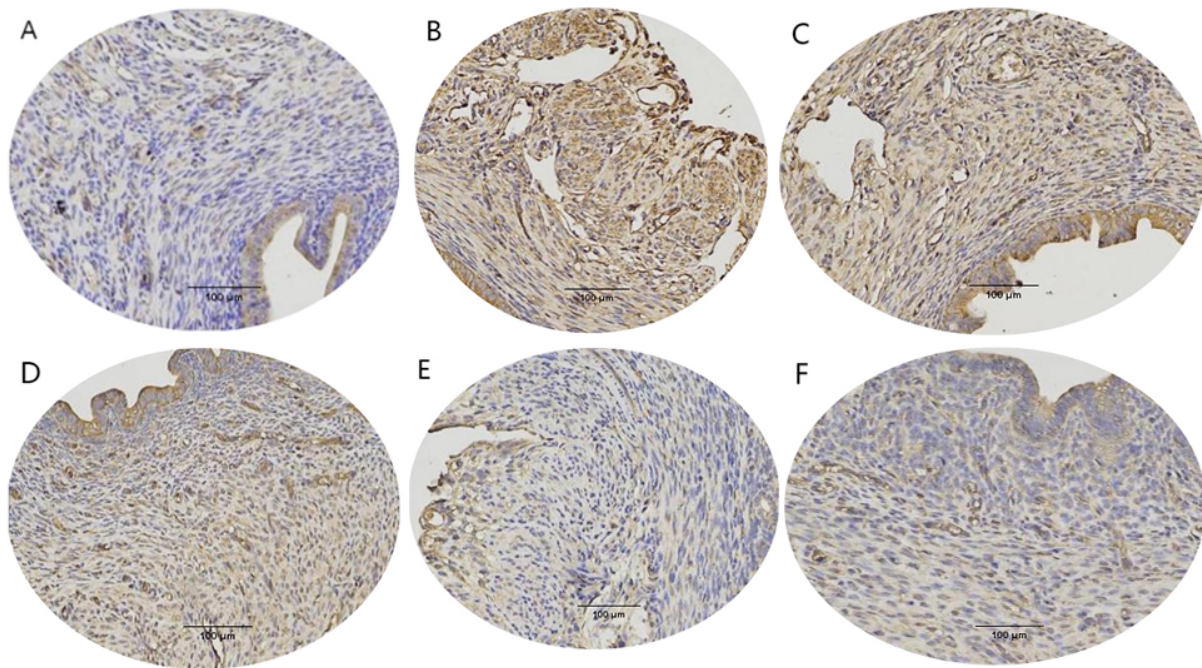


**Fig. 5. Cluster of differentiation 14 (CD14) expression on mice uterus (200×).** (A) Control group. (B) Model group. (C) Low-dose group. (D) Medium-dose group. (E) High-dose group. (F) Levofloxacin HCl group.

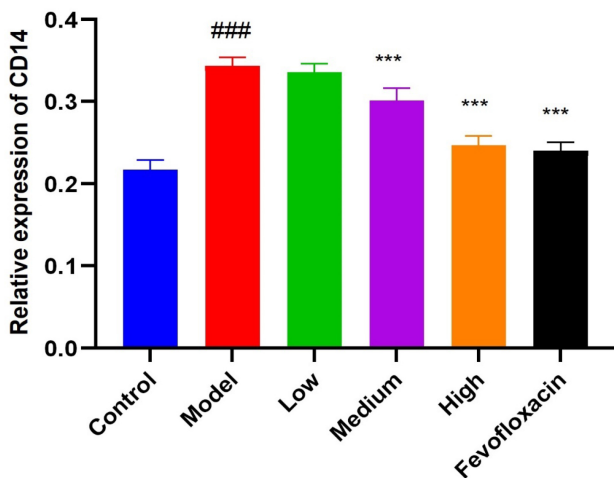


**Fig. 6. Cluster of differentiation 14 (CD14) expression on mice uterus.** Compared with control group (### $p < 0.01$ ). Compared with model group (\*\*\* $p < 0.01$ ).

The gray value of *AQP3* in the model group was significantly ( $p < 0.05$ ) higher compared to the control group. In comparison to the model group, the gray value in the low-dose group was not significantly ( $p > 0.05$ ) changed, while the gray value of *AQP3* in other treatment groups was significantly decreased ( $p < 0.05$ ), as shown in Fig. 8.

### 3.7 Serum Inflammatory Factors in Mice Model

In the model mice group, the serum inflammatory factors (TNF- $\alpha$ , IL-8, IL-6, and IL-1 $\beta$ ) were significantly

higher ( $p < 0.01$ ) compared to the control mice. There was no significant difference ( $p > 0.01$ ) noted between the model group and the low-dose mice. As expected, the content of inflammatory factors in the medium- and high dose groups, as well as the western medicine group, decreased significantly ( $p < 0.01$ ) compared to the model group. However, the content of the anti-inflammatory factor IL-10 was negatively correlated with the inflammatory response. It was significantly lower ( $p < 0.01$ ) in the model group compared to the control group. There was no statistical significance noted between the model group and the low-dose group. The other treatment groups showed significant higher levels of IL-10 compared to the model mice group (Table 4).

### 3.8 Expression of Pyroptosis Related Factor mRNA and Key mRNA of TLR4/NF- $\kappa$ B Signaling Pathway

In comparison to the control mice (Fig. 9), the relative mRNA expression of key genes related to pyroptosis, such as GSDMD, NLRP3, Caspase-1 mRNA, together with p-p65, and TLR4 mRNA in the TLR4 signaling pathway in the model group (with damp heat endometritis induced by multiple factors) were significantly increased ( $p < 0.01$ ). However, the expression of p65 mRNA in each group was not statistically significant ( $p > 0.05$ ). There was no significant difference ( $p > 0.05$ ) between the model group and the low-dose group in the mRNA expression of cell pyroptosis and the TLR4/NF- $\kappa$ B signaling pathway. The expression of p-p65 and TLR4 in the medium-dose group was significantly decreased ( $p < 0.05$ ), but the expression of other

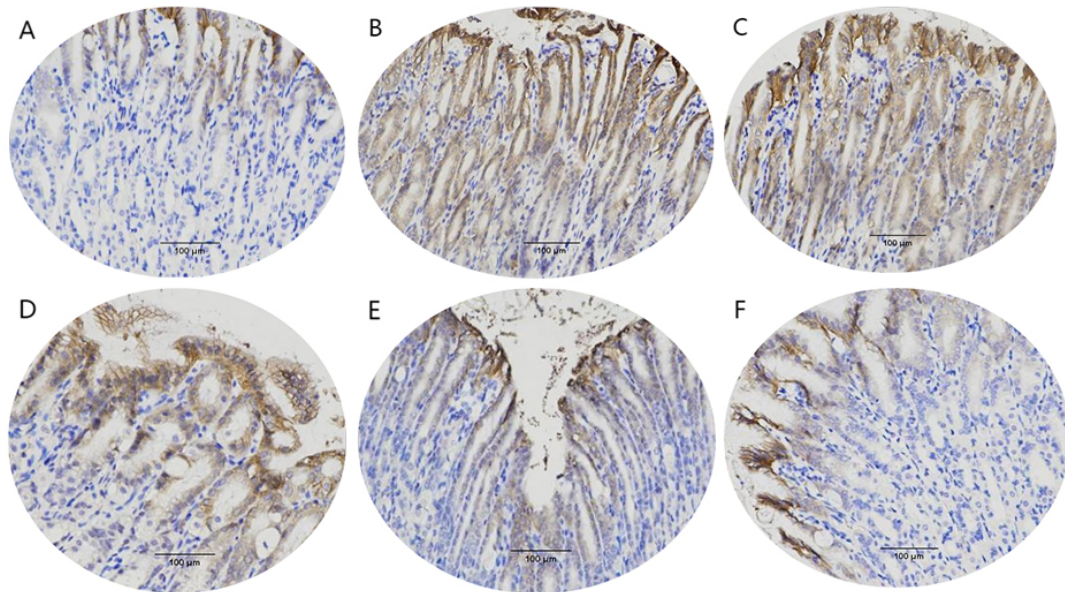


**Fig. 7. Aquaporin 3 (AQP3) expression in mice stomach (200×).** (A) Control group. (B) Model group. (C) Low-dose group. (D) Medium-dose group. (E) High-dose group. (F) Levofloxacin HCl group.

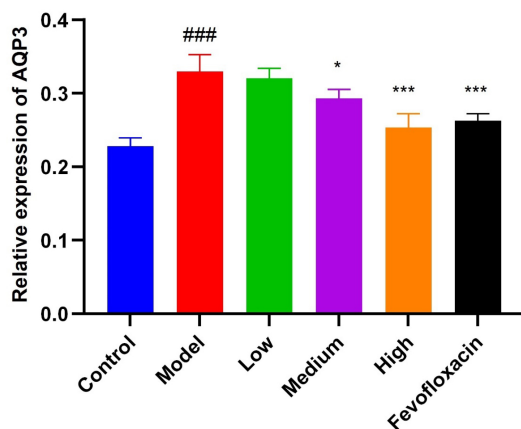


**Fig. 8. AQP3 expression in mice stomach.** Compared with control group (###  $p < 0.01$ ). Compared with model group (\*  $p < 0.05$ , \*\*\*  $p < 0.01$ ).

genes in the medium-dose group was not statistically significant ( $p > 0.05$ ). The relative expression of genes in the two signal pathways decreased significantly ( $p < 0.05$ ) in the high-dose group and western medicine group.

### 3.9 Protein Expression of Pyroptosis-Related Factor mRNA and Key mRNA of TLR4/NF- $\kappa$ B Signaling Pathway

The expression of GSDMD, NLRP3, Caspase-1, Caspase-1p20, TLR4, and p-p65/p65, which are key proteins in the pyrolytic signaling pathway and TLR4/NF- $\kappa$ B signaling pathway, was significantly higher in the model group ( $p < 0.01$ ) compared to the control mice group (Fig. 10). Compared with the model group, the expression of all proteins in the low-, medium-, and high-dose

groups and the Levofloxacin HCl group decreased to varying degrees ( $p < 0.05$ ). Among them, the expression of NLRP3 and caspase-1 in the low-dose group decreased significantly ( $p < 0.05$ ), while the decrease in other proteins was not statistically significant ( $p > 0.05$ ). The effect of Tiaoqi Jiedu formula on endometritis was observed to be dose-dependent.

## 4. Discussion

A study has shown that the main cause of CE is a common bacterial infection, and LPS is the main component [18]. Meanwhile, LPS is related to abortion and premature birth, and its mechanism may be related to its ability to regulate the release of pro-inflammatory factors, such as TNF- $\alpha$  by macrophages, T-cells, and natural killer (NK) cells in the endometrium [19,20]. In addition, LPS can act on luteal cells cultured *in vitro*, thereby affecting multiple functions of the ovary [21]. In traditional Chinese medicine, CE is classified into the categories of “leucorrhea disease” and “infertility”. Many Chinese medicine experts and great traditional Chinese medicine masters believe that the etiology is multifaceted, and the pathogenesis is complex. It is mainly caused by dampness, which is divided into internal dampness and external dampness [22–24]. The internal dampness is mainly attributed to the spleen due to congenital spleen deficiency, improper diet, or excessive fatigue that induces insufficient spleen yang, which is unable to transport water dampness and damages the belt channel. However, external dampness is mainly due to humid climates and living in wetlands for a long time, which can eventually lead to diseases such as pelvic inflammation, infertility, and others [25,26].

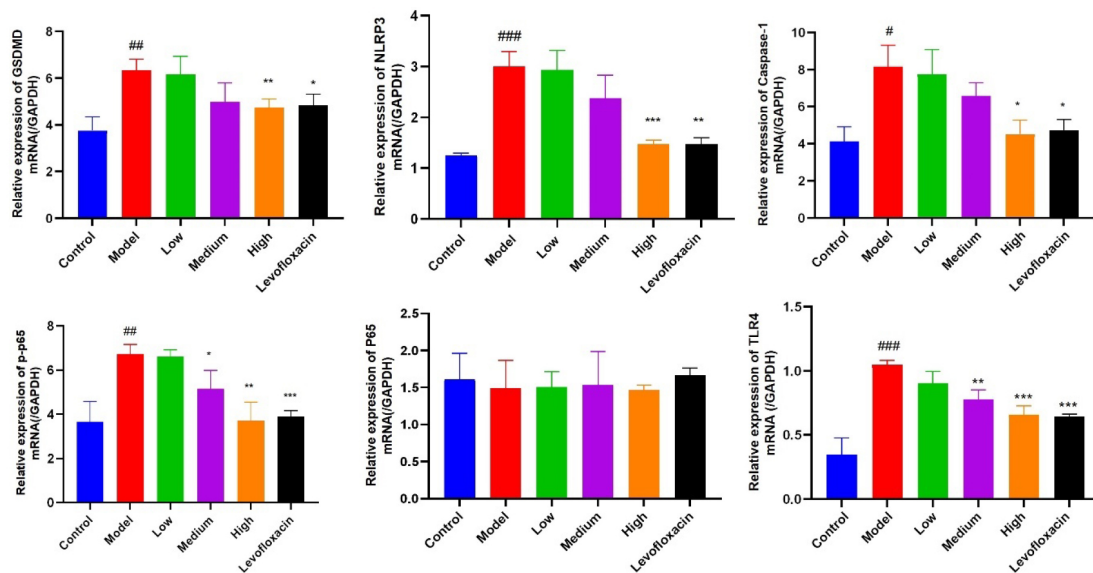


**Fig. 9.** mRNA expression of pyroptosis related factor GSDMD, NLRP3, Caspase-1 and key factor of TLR4/nuclear factor- $\kappa$ B (NF- $\kappa$ B) signalling pathway on mice uterus. Compared with control group ( $^{\#}p < 0.05$ ,  $^{\#\#}p < 0.01$ ,  $^{\#\#\#}p < 0.001$ ). Compared with model group ( $^*p < 0.05$ ,  $^{**}p < 0.01$ ,  $^{***}p < 0.001$ ).

Our research group has, for the first time, constructed for the first time, a mouse model of endometritis induced by dampness, heat, and multiple factors. This model simulates the pathogenic mechanisms of both TCM syndrome and Western medicine. As external reference indices of excess heat syndrome, we observed physical appearance and pathological sections. For the internal indices of the dampness heat syndrome model, we examined the expression of gastric AQP3 immunohistochemistry.

At the same time, we also established the model of endometritis with dampness heat, by combining it with an intrauterine injection of LPS. In terms of TCM syndromes, the appearance of the mice, such as mental malaise, little movement, loose stool, and tongue, was consistent with clinical observations. Meanwhile, the AQP3 in the model group was significantly increased, and there were changes after treatment. The expression of the LPS receptor CD14 in immunohistochemistry and HE staining of the uterus, jointly confirms that our model construction was successful, and the treatment of gynecological Qi regulating and detoxifying formula was effective.

The composition of the gynecological Tiaoqi Jiedu formula includes fifteen traditional Chinese medicines and Zhuang medicines. It reduces heat, detoxifies, and strengthens the spleen, and eliminates dampness, improves liver function (with a soothing effect), and fixes astringency. Among them, the principal drugs are Huanghua Daoshuilian and Wuzhi Maotao, which are medicinal materials, homologous to drug food [27,28]. Studies have shown that the main active components of Huanghua Daoshuilian (also known as polygala) are saponins and flavonoids [29–31]. Saponins exhibit anti-inflammatory and immune-regulating

effects. By inhibiting the activation of the NF- $\kappa$ B signaling pathway mediated by TLR4, they can completely prevent the release of inflammatory factors TNF- $\alpha$ , IL-6, and IL-2 stimulated by LPS, without affecting cell function [32–34]. While flavones can significantly inhibit the activation of TNRP3 and reduce the release of inflammatory factors, such as IL-1 $\beta$  and IL-8 to prevent cell death and protect the endometrium [35,36]. The results of this study show that different concentrations of the gynecological Tiaoqi Jiedu formula can down-regulate the protein expression and mRNA in pyroptosis and TLR4/NF- $\kappa$ B signaling pathways, such as GSDMD, NLRP3, Caspase-1, TLR4, p-p65, and proteins to varying degrees. At the same time, in the ELISA results, the gynecological Tiaoqi Jiedu formula can significantly reduce the contents of pro-inflammatory factors IL-6, IL-1 $\beta$ , IL-8, and TNF- $\alpha$  and increase the content of IL-10, which was positively correlated with the concentration.

In the 2015 edition of the Chinese Pharmacopoeia, there are three types of Chinese patent medicines containing Wuzhi Maotao, which are used to treat gynecological diseases: Gongyanping dropping pills, Fuyanjing capsules, and Gongyanping tablets. Numerous studies have shown that quercetin, an effective active ingredient in Wuzhi Maotao [37], can regulate inflammatory factors, growth factors, and signal pathways [38], leading to anti-inflammatory, anti-cancer, anti-oxidation, and immune-regulating effects [27,39–41]. Quercetin has a similar structure to mammalian estrogen and can regulate estrogen receptors with high affinity. By regulating estrogen receptors [42], inhibiting the release of inflammatory factors, and regulating the endometrial microenvironment, quercetin can improve the pregnancy rate and protect the fetus. Thus, it explains the

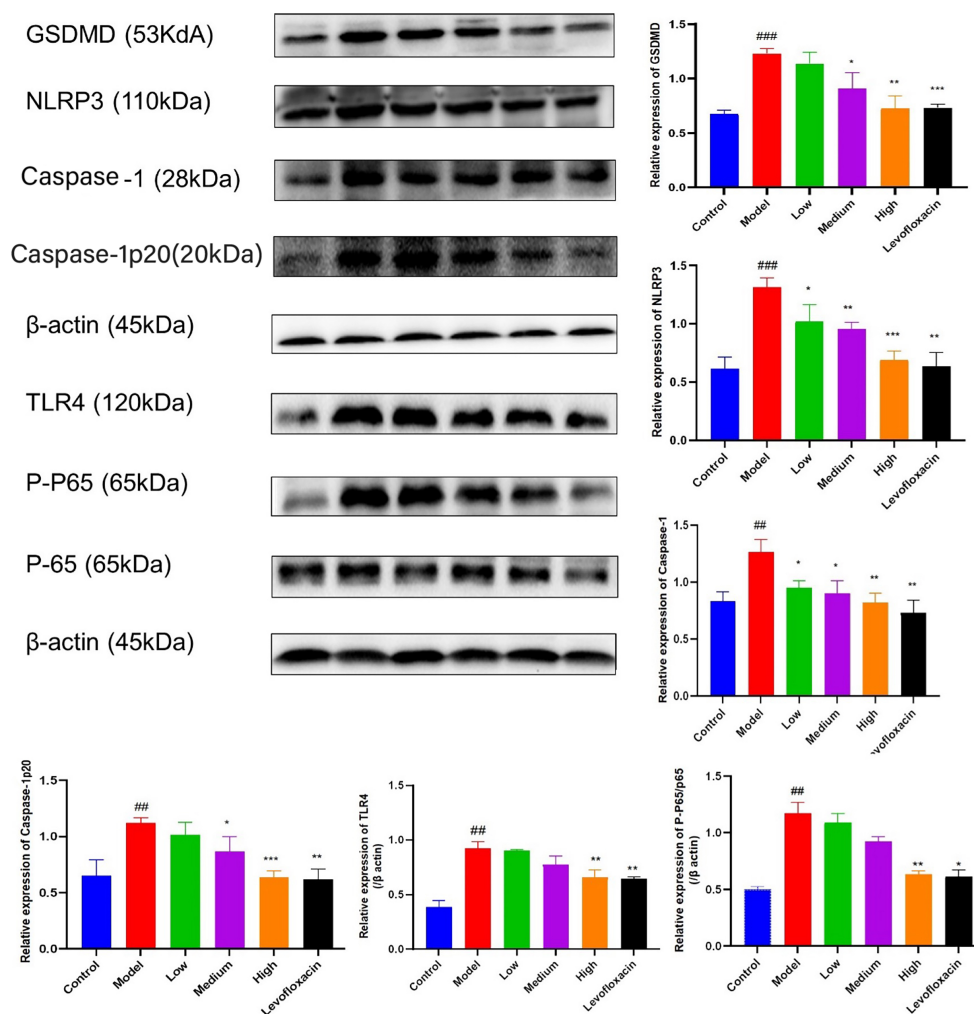


**Fig. 10. Expression of key proteins in pyroptosis and TLR4/NF- $\kappa$ B signalling pathway, and statistical analysis.** Compared with control group (## $p < 0.01$ , ### $p < 0.001$ ). Compared with model group (\* $p < 0.05$ , \*\* $p < 0.01$ , \*\*\* $p < 0.001$ ).

effect of gynecological Tiaoqi Jiedu formula in improving menstruation and increasing the probability of pregnancy, while treating endometritis with dampness and heat.

## 5. Conclusions

The study demonstrated that the Tiaoqi Jiedu formula was effective in treating endometritis with dampness and heat through multiple channels, and multiple targets. However, the reader should note the limitations of this study, which is the difference between animal and human bodies. In the future, the effect of Tiaoqi Jiedu formula on improving menstruation and pregnancy needs to be studied. The present study lays a solid foundation for future experiments involving human endometrial stromal cells. It also provides a fresh perspective and basis for protecting the endometrium and improving the pregnancy rate while treating CE.

## Abbreviations

AQP3, Aquaporin 3; CD14, Cluster of differentiation 14; IL, Interleukin; TNF, Tumor necrosis factor; ELISA, Enzyme-Linked Immunosorbent Assay; NLRP3, NOD-, LRR- and pyrin domain-containing protein 3; GSDMD, Gasdermin D; TLR4, Toll-like receptor 4; NF- $\kappa$ B, Nuclear factor- $\kappa$ B; CE, Chronic endometritis; TCM, Traditional Chinese Medicine; SPF, Specific pathogen free; CASP1, Cysteine-aspartic acid protease; SABC, Streptavidin-Biotin complex; BCA, bicinchoninic acid; SPSS, Statistical Package for the Social Sciences.

## Availability of Data and Materials

Data will be available on request.

## Author Contributions

JC designed the research study; JC and CZ performed ELISA, Real-time PCR, Western Blot, Immunohistochemi-

cal staining, and HE staining experiments; WY and YL analyzed the data and performed research; NL were involved in formal analysis and funding. All authors contributed to editorial changes in the manuscript. All authors read and approved the final manuscript. All authors have participated sufficiently in the work and agreed to be accountable for all aspects of the work.

## Ethics Approval and Consent to Participate

The study was performed according to the guidelines of “Animal Quality Management Measures” issued by the State Science and Technology Commission. The animals were approved by the Ethics Committee of “The Guangxi International Zhuang Medicine Hospital” (approval number: DW2020127-200).

## Acknowledgment

Thanks to Guangxi University of Traditional Chinese Medicine for the experimental equipment and venue. Thanks to Dr. Xiaoyun Zhang who gave guidance during the experiment. Thanks to the teachers who helped in the process of writing the paper. Thanks to all the peer reviewers for their opinions and suggestions.

## Funding

This study was supported by Introduction of Talent Research Startup foundation of Guangxi International Zhuang Medicine Hospital (GZ2021RC012); Administration of Traditional Chinese Medicine of Guangxi Zhuang Autonomous Region in 2021 (GXZYZ20210172); “High-level Talent Cultivation and Innovation Team” Project of Guangxi University of Chinese Medicine (No:2022A008); The State Administration of Traditional Chinese Medicine “Twelfth Five-Year” Key Discipline of Traditional Chinese Medicine National Pharmacy (Zhuang Pharmacy); Guangxi Traditional Chinese Medicine Multidisciplinary Innovation Team Project.

## Conflict of Interest

The authors declare no conflict of interest.

## References

- [1] Puente E, Alonso L, Laganà AS, Ghezzi F, Casarin J, Carugno J. Chronic Endometriosis: Old Problem, Novel Insights and Future Challenges. *International Journal of Fertility & Sterility*. 2020; 13: 250–256.
- [2] Molina NM, Sola-Leyva A, Saez-Lara MJ, Plaza-Diaz J, Tubić-Pavlović A, Romero B, *et al*. New Opportunities for Endometrial Health by Modifying Uterine Microbial Composition: Present or Future? *Biomolecules*. 2020; 10: 593.
- [3] Kimura F, Takebayashi A, Ishida M, Nakamura A, Kitazawa J, Morimune A, *et al*. Review: Chronic endometriosis and its effect on reproduction. *The Journal of Obstetrics and Gynaecology Research*. 2019; 45: 951–960.
- [4] Buzzaccarini G, Vitagliano A, Andrisani A, Santarsiero CM, Cincinelli R, Nardelli C, *et al*. Chronic endometriosis and altered embryo implantation: a unified pathophysiological theory from a

- literature systematic review. *Journal of Assisted Reproduction and Genetics*. 2020; 37: 2897–2911.
- [5] Takebayashi A, Kimura F, Kishi Y, Ishida M, Takahashi A, Yamanaoka A, *et al*. The association between endometriosis and chronic endometriosis. *PLoS ONE*. 2014; 9: e88354.
- [6] Cueva F, Caicedo A, Hidalgo P. A Need for Standardization of the Diagnosis and Treatment of Pelvic Inflammatory Disease: Pilot Study in an Outpatient Clinic in Quito, Ecuador. *Infectious Diseases in Obstetrics and Gynecology*. 2020; 2020: 5423080.
- [7] Xiong Y, Chen Q, Chen C, Tan J, Wang Z, Gu F, *et al*. Impact of oral antibiotic treatment for chronic endometritis on pregnancy outcomes in the following frozen-thawed embryo transfer cycles of infertile women: a cohort study of 640 embryo transfer cycles. *Fertility and Sterility*. 2021; 116: 413–421.
- [8] Farshchi M, Abdollahi E, Saghafi N, Hosseini A, Fallahi S, Rostami S, *et al*. Evaluation of Th17 and Treg cytokines in patients with unexplained recurrent pregnancy loss. *Journal of Clinical and Translational Research*. 2022; 8: 256–265.
- [9] Huang Y, HUANG C. Traditional Chinese functional foods. *Asian Foods: Science and Technology*. 1999; 409–452.
- [10] Zhang S, Yuan L, Wang Y, Sun Z. Effect of Fu Yan Qing prescription on pelvic effusion, mass absorption and microenvironment of pelvic blood stasis in patients with sequelae of pelvic inflammatory disease of accumulation of dampness heat and blood stasis type. *Pakistan Journal of Medical Sciences*. 2022; 38: 1376.
- [11] Qu F, Zhou J, Ma B. The effect of Chinese herbs on the cytokines of rats with endometriosis. *Journal of Alternative and Complementary Medicine (New York, N.Y.)*. 2005; 11: 627–630.
- [12] Li W, Fu K, Lv X, Wang Y, Wang J, Li H, *et al*. Lactoferrin suppresses lipopolysaccharide-induced endometritis in mice via down-regulation of the NF-κB pathway. *International Immunopharmacology*. 2015; 28: 695–699.
- [13] Naqvi H, Mamillapalli R, Krikun G, Taylor HS. Endometriosis Located Proximal to or Remote From the Uterus Differentially Affects Uterine Gene Expression. *Reproductive Sciences (Thousand Oaks, Calif.)*. 2016; 23: 186–191.
- [14] Kadhim KK, Zuki A, Babjee A, Noordin M, Zamri-Saad M. Morphological and histochemical observations of the red jungle fowl tongue *Gallus gallus*. *African Journal of Biotechnology*. 2011; 10: 9969–9977.
- [15] Kalof AN, Cooper K. Our approach to squamous intraepithelial lesions of the uterine cervix. *Journal of Clinical Pathology*. 2007; 60: 449–455.
- [16] Ohno S, Ohno Y, Suzuki N, Kamei T, Koike K, Inagawa H, *et al*. Correlation of histological localization of tumor-associated macrophages with clinicopathological features in endometrial cancer. *Anticancer Research*. 2004; 24: 3335–3342.
- [17] Bagaria V, Mathur P, Madan K, Kumari M, Sagar S, Gupta A, *et al*. Predicting Outcomes After Blunt Chest Trauma-Utility of Thoracic Trauma Severity Score, Cytokines (IL-1β, IL-6, IL-8, IL-10, and TNF-α), and Biomarkers (vWF and CC-16). *The Indian Journal of Surgery*. 2021; 83: 113–119.
- [18] Kitaya K, Takeuchi T, Mizuta S, Matsubayashi H, Ishikawa T. Endometriosis: new time, new concepts. *Fertility and Sterility*. 2018; 110: 344–350.
- [19] Hussain T, Tan B, Liu G, Murtaza G, Rahu N, Saleem M, *et al*. Modulatory Mechanism of Polyphenols and Nrf2 Signaling Pathway in LPS Challenged Pregnancy Disorders. *Oxidative Medicine and Cellular Longevity*. 2017; 2017: 8254289.
- [20] Hirata Y, Shimazaki S, Suzuki S, Henmi Y, Komiyama H, Kuwayama T, *et al*. β-hydroxybutyrate suppresses NLRP3 inflammasome-mediated placental inflammation and lipopolysaccharide-induced fetal absorption. *Journal of Reproductive Immunology*. 2021; 148: 103433.
- [21] Terranova PF, Rice VM. Review: cytokine involvement in ovar-

- ian processes. *American Journal of Reproductive Immunology* (New York, N.Y.: 1989). 1997; 37: 50–63.
- [22] Das M. WHO launches strategy to accelerate elimination of cervical cancer. *The Lancet. Oncology*. 2021; 22: 20–21.
- [23] Mao P, Liu S, Xue J, Wu Y, Wang C. Clinical research on the comprehensive curative effect of acupuncture and traditional Chinese medicine for pelvic inflammatory sequelae. *Medical science monitor*. 2018; 24: 2928.
- [24] Zhang Y, Zhao Z, Chen H, Fu Y, Wang W, Li Q, *et al.* The underlying molecular mechanisms involved in traditional Chinese medicine *Smilax china L.* for the treatment of pelvic inflammatory disease. *Evidence-based Complementary and Alternative Medicine*. 2021; 2021.
- [25] World Health Organization. Regional Office for the Western Pacific. WHO International Standard Terminologies on Traditional Medicine in the Western Pacific Region. World Health Organization. 2007.
- [26] Yang M, Zhao Y. Cui Yuheng's experience of 8 treatment methods in the treatment of leukorrhea diseases. *China Journal of Traditional Chinese Medicine and Pharmacy*. 2018; 33: 3965–3969. (In Chinese)
- [27] Ye T, Wu YW, Shi RJ, Wu YW, Wu YH, Li YX. Advances in the Study on the Chemical Composition and Pharmacological Activity of Radix Fici Simplicissimae. *Journal of Guangdong Pharmaceutical University*. 2019; 35: 591–596. (In Chinese)
- [28] Tian E, Liu Q, Ye H, Li F, Chao Z. A DNA barcode-based RPA assay (BAR-RPA) for rapid identification of the dry root of *Ficus hirta* (Wuzhimaotao). *Molecules*. 2017; 22: 2261.
- [29] Cheng YG, Tan JY, Li JL, Wang SH, Liu KL, Wang JM, *et al.* Chemical constituents from the aerial part of *Polygala tenuifolia*. *Natural Product Research*. 2022; 36: 5449–5454.
- [30] Çalış İ, Ünlü A, Uğurlu Aydın Z, Dönmez AA, Soliman Yusufoglu H, Jurt S, *et al.* Xanthones and Xanthone O-β-D-Glucosides from the Roots of *Polygala azizsancarii* Dönmez. *Chemistry & Biodiversity*. 2022; 19: e202200499.
- [31] Chen Z, Yang Y, Han Y, Wang X. Neuroprotective effects and mechanisms of senegenin, an effective compound originated from the roots of *polygala tenuifolia*. *Frontiers in Pharmacology*. 2022; 13: 937333.
- [32] Yang SP, Xiu MH, Liu YQ, Yang XQ, Yang FJ. Research Progress on anti-aging mechanism of Chinese medicine saponins. *Chinese Journal of Gerontology*. 2022; 42: 3327–3335.
- [33] Li TZ, Zhang WD, Yang GJ, Liu WY, Chen HS, Shen YH. Saponins from *Polygala japonica* and their effects on a forced swimming test in mice. *Journal of Natural Products*. 2006; 69: 591–594.
- [34] Yan WF, Shao QH, Zhang DM, Yuan YH, Chen NH. The molecular mechanism of polygalasaponin F-mediated decreases in TNFα: emphasizing the role of the TLR4-PI3K/AKT-NF-κB pathway. *Journal of Asian Natural Products Research*. 2015; 17: 662–670.
- [35] Ruiz P A, Haller D. Functional diversity of flavonoids in the inhibition of the proinflammatory NF-κB, IRF, and Akt signaling pathways in murine intestinal epithelial cells. *The Journal of nutrition*. 2006; 136: 664–671.
- [36] Tsai PJ, Huang WC, Hsieh MC, Sung PJ, Kuo YH, Wu WH. Flavones isolated from *Scutellariae radix* suppress *Propionibacterium acnes*-induced cytokine production in vitro and in vivo. *Molecules*. 2015; 21: 15.
- [37] Qin RH, Pan Y, Chen RX, Deng YP, Liu XF. HPLC method for simultaneous determination of six flavonoids in radix *fici simplicissimae*. *Chinese Journal of Pharmaceutical Analysis*. 2020; 40: 2244–2249. (In Chinese)
- [38] Kashyap D, Garg VK, Tuli HS, Yerer MB, Sak K, Sharma AK, *et al.* Fisetin and Quercetin: Promising Flavonoids with Chemopreventive Potential. *Biomolecules*. 2019; 9: 174.
- [39] Ye X, Tian W, Wang G, Zhang X, Zhou M, Zeng D, *et al.* Phenolic glycosides from the roots of *Ficus hirta* vahl. And their antineuroinflammatory activities. *Journal of agricultural and food chemistry*. 2020. 68: 4196–4204.
- [40] Zeng Y, Liu X, Lv Z, Peng Y. Effects of *Ficus hirta* Vahl.(Wuzhimaotao) extracts on growth inhibition of HeLa cells. *Experimental and toxicologic pathology*. 2012; 64: 743–749.
- [41] Tang SM, Deng XT, Zhou J, Li QP, Ge XX, Miao L. Pharmacological basis and new insights of quercetin action in respect to its anti-cancer effects. *Biomedicine & Pharmacotherapy = Biomedecine & Pharmacotherapie*. 2020; 121: 109604. (In Chinese)
- [42] Bandera EV, Williams MG, Sima C, Bayuga S, Pulick K, Wilcox H, *et al.* Phytoestrogen consumption and endometrial cancer risk: a population-based case-control study in New Jersey. *Cancer Causes & Control: CCC*. 2009; 20: 1117–1127.